ACS OMEGA

http://pubs.acs.org/journal/acsodf

Article

Voltammetric Determination of Hg^{2+}, Zn^{2+}, and Pb^{2+} Ions Using a PEDOT/NTA-Modified Electrode

Jasim M. S. Alshawi, Mohammed Q. Mohammed,* Hasan F. Alesary,* Hani K. Ismail, and Stephen Barton

Cite This: *ACS Omega* 2022, 7, 20405−20419

Read Online

ACCESS | Metrics & More | Article Recommendations

ABSTRACT: A novel electrochemical sensor for determining trace levels of Hg^{2+}, Pb^{2+}, and Zn^{2+} ions in water using square wave voltammetry (SWV) is reported. The sensor is based on a platinum electrode (Pt) modified by poly(3,4-ethylenedioxythiophene) and N_{α},N_{α}-bis-(carboxymethyl)-L-lysine hydrate (NTA lysine) PEDOT/NTA. The modified electrode surface (PEDOT/NTA) was prepared via the introduction of the lysine-NTA group to a PEDOT/N-hydroxyphthalimide NHP electrode. The (PEDOT/NTA) was characterized via cyclic voltammetry (CV), Fourier transform infrared (FTIR) spectroscopy, and scanning electron microscopy (SEM). The effects of scan rates on the electrochemical properties of the polymer electrode were also investigated. The electrochemical results were used to estimate the coverage of the electrode polymer surface and its electrostability in background electrolyte solutions. Several analytical parameters, such as polymer film thickness, metal deposition time, and pH of the electrolyte, were examined. Linear responses to Hg^{2+}, Pb^{2+}, and Zn^{2+} ions in the concentration range of 5−100 μg L^{-1} were obtained. The limits of detection (LODs) for the determination of Hg^{2+}, Pb^{2+}, and Zn^{2+} ions were 1.73, 2.33, and 1.99 μg L^{-1}, respectively. These promising results revealed that modified PEDOT/NTA films might well represent an important addition to existing electrochemical sensor technologies.

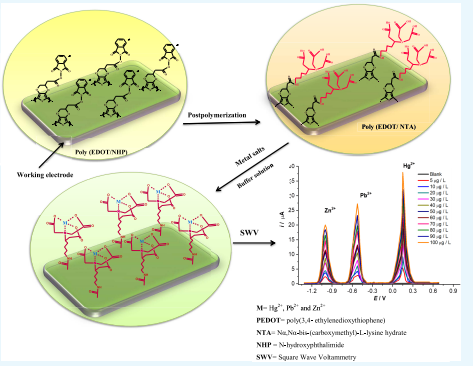

1. INTRODUCTION

Environmental contamination from metals such as zinc, cadmium, lead, copper, cobalt, nickel, and mercury is a serious concern even at trace concentrations,[1−3] requiring the development of sensitive, selective, and accurate analytical methods to monitor such species.[4] To date, many diverse techniques have been used for their detection, such as absorption,[5] emission,[6] fluorescence spectrometry,[7] optical techniques, atomic absorption,[8] and electrochemical technologies.[9−11] Electroanalytical methods are considered an efficient means of detecting a broad range of organic, inorganic, and heavy-metal ions because of their high accuracy, adaptability, sensitivity, rapid responses, and the fact that they are relatively inexpensive.[12−14]

Accumulation of these heavy metals can lead to serious damage to organs such as the liver and kidneys and further to conditions such as anemia, respiratory disorders, cancers, lung damage, digestive issues, and osteomalacia.[15] World organizations like the WHO state that the highest allowable concentrations of Hg^{2+}, Pb^{2+}, and Zn^{2+} in terms of human exposure are 1, 50, and 5000 μg L^{-1}, respectively.[16−18] Environmental monitoring has become an important issue over recent years as a result of increased public awareness and concern about pollution. This has driven the need to develop sensory tools that are sensitive, selective, portable, and inexpensive. The efficiency of electroactive polymers in this regard has been demonstrated in a number of areas, such as conductometric, potentiometric, amperometric, and chemical sensors.[19,20]

The detection of metal ions using conducting polymers can be improved by modification of electrode surfaces through various chemical methods and functionalization techniques.[23,24] When functional groups are sited on a polymer surface, they can perform various functions such as catalysis, sensing, and chemiluminescence.[21] Furthermore, functionalized surfaces have the smart ability to change their physical and chemical structures on exposure to specific stimuli.[22] This study has focused on the detection of Hg^{2+}, Pb^{2+}, and Zn^{2+} ions using a novel electrochemical sensor based on the modification of polymer electrodes with high sensitivity.[25] The fine-tuning of the chemoanalytical features of polymer electrodes to facilitate interaction with particular analyte species can be accomplished via the introduction of specific

Received: April 30, 2022
Accepted: May 24, 2022
Published: June 1, 2022

Scheme 1. Mechanism Describing the Chemical Synthesis of Poly(EDOT/NHP) via Electrochemical Polymerization

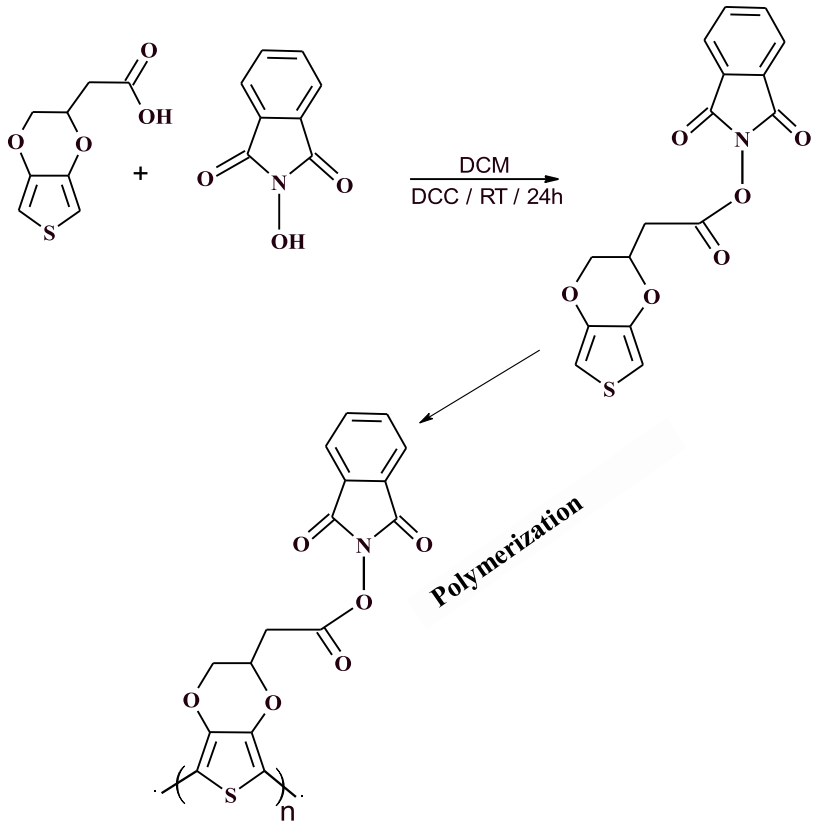

receptor groups into the polymer films that function as metal-ion acceptors.[26]

Electroactive polymers such as polythiophene,[27] polypyrrole,[28] poly(3,4-ethylenedioxythiophene),[29] polyaniline,[30,31] polyfuorene,[32] poly(5-aminoquinoline), poly(*o*-toluidine),[33] and their derivatives have attracted considerable interest.[34] The optical, chemical, electronic, and mechanical features of these polymer films render them suitable candidates for possible applications in chemical sensors,[35] corrosion protection,[36] electrochromic devices,[37] supercapacitors,[38] energy storage,[39] and artificial muscles.[40] Covalent bonding of ligands with the functional groups of the surface polymer film allows the powerful immobilization of particular chemical species. The principal technique used to modify polymer surfaces is via the introduction of receptors/ligands, as reported in the various literature reviews on this subject. Suitable monomers, such as aniline, pyrrole, thiophene, and 3,4-ethylenedioxythiophene (EDOT), when bearing carboxyl groups with alkyl spacers,[41] can be activated via appropriate leaving groups such as pentafluorophenol (PFP) and *N*-hydroxysuccinimide (NHP).

Functionalization chemistry plays a vital role in the modification and improvement of many of the physical characteristics of polymeric films. Side chains with functional groups on polymer surfaces might be considered analogous to "molecular wires", which can often contribute to facilitating the movement of electrons within electrochemical systems (electrode and electrolytes).[42] Functionalization of polymer film surfaces may also be utilized to improve electrode performance, thereby potentially giving conducting polymers a significantly increased number of applications in various scientific areas such as gas sensors, electronic muscles, energy electrochromic devices, and bioelectronic interfaces. The modification of the electrode structure can have a notable impact on the features of the electrode through the associated effect on the movement of species (molecules or electrons) within the polymer film itself.[43] Chemically modified polymers with end functional groups have been used to enhance metal detection in the aqueous environment. Nitrilotriacetic acid is considered to be an excellent ligand for the binding of metal ions in aqueous solution, similar to ethylenediaminetetraacetic acid (EDTA). Among the many possible organic receptors, nitrilotriacetic acid (NTA) has been found to be one of strongest chelating molecules available.[44] Recently, the *N*-nitrilotriacetic acid receptor system has begun to see common usage in sensor devices and in the biosciences.[26] Further, as a multidentate ligand, it can form a hexagonal complex configuration on reaction with metal ions such as Co, Ni, Cu, Zn, or Cr.

The aim of this project is to modify the chemical structure of surface films and to control the molecular design to enable them to be used for selective detection of metal ions in aqueous solution. To achieve this objective, the present work will investigate the activation of end functional groups on film surfaces to create smart surfaces that have particular analytical functions. The scenario involves electrochemical polymerization of the EDOT/NHP monomer, which contains a good leaving group, namely, pentafluorophenol (PFP). The PFP group provides two advantages: first, it does not inhibit the electropolymerization process, and second, it is easy to substitute this group onto film surfaces without resulting in the collapse of the polymer film itself. After the deposition of the PEDOT/NHP polymer, the ester bonds can be hydrolyzed

https://doi.org/10.1021/acsomega.2c02682
ACS Omega 2022, 7, 20405−20419

Scheme 2. Postpolymerization Step and Synthesis of PEDOT/NTA

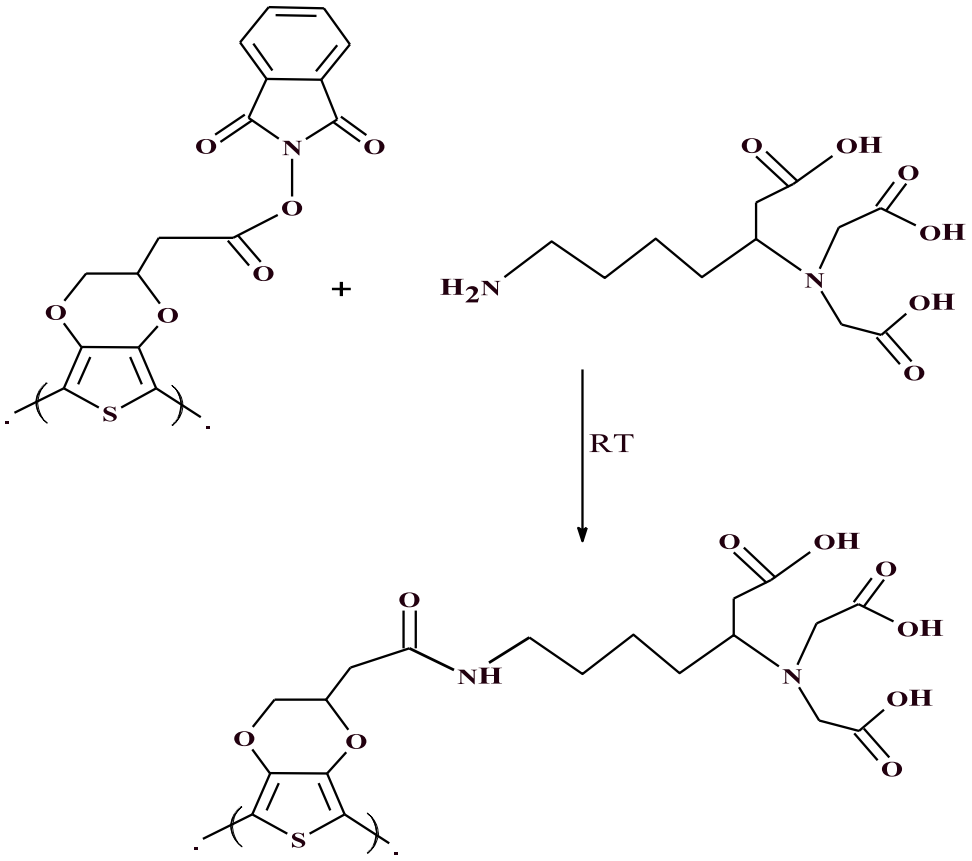

to produce convenient voids for the subsequent insertion of ligand groups (NTA).

In this study, the polymer films under investigation are based on electrochemical polymerization of the EDOT monomer derivatives, PEDOT/NHP, and PEDOT/NTA (Schemes 1 and 2), where the NHP polymer film can be modified to create a PEDOT/NTA film via reaction with nucleophilic molecules in solution under mild conditions. Postpolymerization methods allow for the formation of new functionalized film surfaces and also prevent the surface from collapsing. NTA lysine has been used to graft PFP polymer surfaces to form "ligand" chemical sensors. In this research paper, we report a novel electrochemical sensor that utilizes NTA lysine, covalently bonded to a poly(EDOT) film and mounted onto a platinum electrode for detection of trace amounts of contaminant metals in aqueous samples. The novel poly-(EDOT/NTA)-modified electrode so produced demonstrated excellent efficiency in detecting low concentrations of Hg^{2+}, Pb^{2+}, and Zn^{2+} ions in water.

2. EXPERIMENTAL SECTION

2.1. Chemical Materials. 2-Carboxymethyl-3,4-ethylenedioxythiophene (EDOT-MeCOOH), tetrabutylammonium perchlorate (TBAP) (99%), N_{α},N_{α}-bis(carboxymethyl)-L-lysine (NTA), and *N*-hydroxyphthalimide (97%) were purchased from Sigma-Aldrich. Dicyclohexylcarbodiimide (DCC) and magnesium sulfate were purchased from Thermo Fisher Scientific. Dichloromethane (CH_2Cl_2) was purchased from Tianjin Damao Chemical Reagent Factory. Tetrabutylammonium perchlorate 99% (TBAP) was purchased from Acros Organics (and was further dried under vacuum at 60 °C for 1 day before use). The preparation of an acetate buffer solution was accomplished using 0.2 M acetic acid (CH_3COOH) with 0.2 M sodium acetate (CH_3COONa) to reach the desired pH. Pure water solvent was used for the processes that required an aqueous medium.

2.2. Instruments. Electrochemical examinations (square wave voltammetry (SWV) and cyclic voltammetry (CV)) were achieved using a PGSTAT-20 potentiostat from ECO/Chemie (The Netherlands). The measurements were typically accomplished using a three-electrode system containing a working, counter, and reference electrode. The platinum electrode (area = 0.75 mm^2) was used as the working electrode (WE). The Pt plate (2.5 mm^2) was used as the counter electrode, and an Ag/AgCl system was used as the reference electrode. The electrodeposition of EDOT-NHP (monomer) on WE was carried out via cyclic voltammetry. FTIR spectra of polymer films were recorded using a PerkinElmer Frontier FTIR spectrophotometer (Massachusetts). An FEI SIRION scanning electron microscopy device was employed to examine the morphologies of the electrode surfaces deposited on the platinum electrodes. Cyclic voltammetry was utilized for the electropolymerization of the EDOT/NHP monomer. The voltage range was swept 10 times between −0.9 and 1.2 V at various scan rates (10−100 mV s^{-1}). The appearance of polymer films on electrode surfaces was evident from the formation of a dark color on the WE. The deposited film was washed using ultrapure water and acetone to remove excess unreacted monomer from the film surface and then dried.

2.3. Preparation of Standard Solutions. Stock solutions (with 100 ppm concentrations) were prepared by dissolving

https://doi.org/10.1021/acsomega.2c02682
ACS Omega 2022, 7, 20405−20419

each of the selected metal ions in ultrapure water. A solution of Pb ions was synthesized by dissolving 0.1598 g of lead nitrate ($Pb(NO_3)_2$) in deionized water and then diluting to 1000 mL. The mercury and zinc solutions were similarly produced by dissolving 0.1623 g of $Hg(NO_3)_2$ and 0.2084 g of $ZnCl_2$, in ultrapure water and then diluting to 1000 mL. Prepared standard solutions were utilized to make a set of solutions with concentrations varying from 1 to 100 ppm for selected ions.

2.4. Synthesis of PEDOT/NHP Monomer. The monomer (EDOT/NHP) was prepared via esterification of the carboxylic group of EDOT/COOH with *N*-hydroxyphthalimide (NHP) and dicyclohexylcarbodiimide (DCC). This procedure can be summarized as follows: a solution of DCC (9.07 g, 44 mmol) and NHP (7.17 g, 44 mmol) in dry DCM (75 mL) was added to a stirred solution of EDOT/COOH (8.01 g, 44 mmol) in dry DCM (20 mL). The reaction mixture was stirred for 24 h. The white precipitate (dicyclohexylurea) that subsequently formed was isolated, and the DCM solvent was removed from solution under vacuum to obtain the crude product. This yield was recrystallized in hexane, filtered off, and dried under vacuum (85%). The associated chemical reaction scheme is shown in Scheme 1.

2.5. Electropolymerization of PEDOT/NHP. The EDOT/NHP monomer that was prepared via an esterification reaction in the previous step was electropolymerized in a suitable electrolyte to produce an electroactive polymer film containing an activated ester group. Voltammetric polymerization was performed on a platinum electrode using a reaction solution containing 10 mM EDOT/NHP with 0.1 M tetrabutylammonium perchlorate (TBAP) in CH_2Cl_2 (DCM). The potential was cycled between −0.9 V and 1.2 V vs RE (Ag/AgCl) and the PEDOT/NHP film was coated on the platinum electrode for 10 consecutive scans with increasing redox peak currents. The modified electrode thus produced will be referred to herein as a PEDOT/NHP electrode.

2.6. Postpolymerization and Preparation of PEDOT/NTA. The postpolymerization polymer film, which was converted to an activated ester via a hydrolysis reaction, was then bound with NTA groups within the polymer film. The next step was to study the physical and chemical stabilities of the polymer films so produced. This strategy involves the electropolymerization of an EDOT/NHP film containing a reactive ester group that can be replaced by new group after deposition. An amidation reaction was used to bond the NTA groups to the functionalised film (PEDOT/NHP) surface. FTIR spectra were recorded to provide qualitative evidence as to the covalent binding between the functionalized electrode surfaces and ligand units. The introduction of NTA units to the electroactive PEDOT/NHP polymer films was achieved via their immersion in a saturated solution of the NTA ligand. The modified electrode was removed from the immersion solution after 12 h, washed with pure water, and then dried. The synthesis of PEDOT/NTA is illustrated in Scheme 2.

2.7. Electrodetection of Metal Ions. Electrochemical examinations were accomplished using an (AUTOLAB) analyzer device with a three-electrode cell system, as depicted above. The WE was PEDOT/NTA with Ag/AgCl/saturated KCl as the reference electrode and the platinum counter electrode. Acetate buffer solutions (0.2 M, pH 2−9), which contain diverse concentrations of mercury (II), zinc (II), and lead (II) ions, were utilized as the electrolyte solutions for the actual measurements. Practical experiments were carried out at room temperature, 25 ± 2 °C. The parameters for the square wave voltammetry were as follows: pulse amplitude, 10 mV; initial potential, −0.5 V; and end potential, 1.25 V.

3. RESULTS AND DISCUSSION

3.1. Electrochemical Polymerization of PEDOT/NHP. The EDOT/NHP films were electrosynthesized in CH_2Cl_2 solution containing 0.1 M TBAP as the supporting electrolyte and 10 mM EDOT/NHP monomer, as shown in Figure 1.

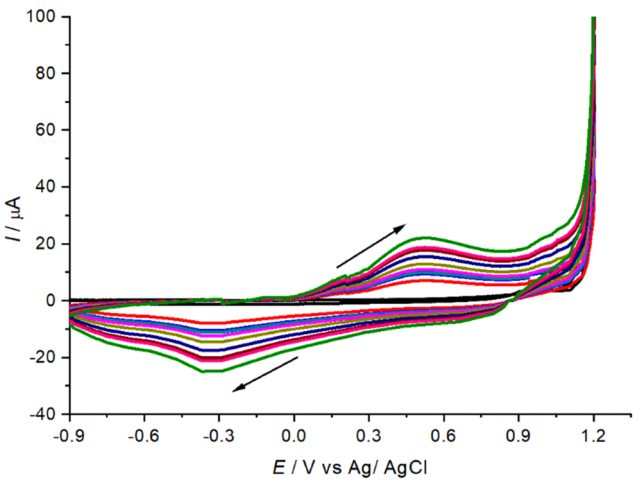

Figure 1. Cyclic voltammograms resulting from electropolymerization of 10 mM monomer (EDOT/NHP) with 0.1 M TBAP in CH_2Cl_2 solution using a potential window of −0.9 to 1.3 V at a scan rate of 10 mV s^{-1} for 10 scans.

The modified polymer film formation on the Pt electrode was characterized by a sharp rise in the current for the voltage at almost 1.05 V vs the Ag/AgCl reference electrode in the cyclic voltammogram of PEDOT/NHP. During electropolymerization, a black layer was formed on the Pt electrode. In addition, a nucleation loop could clearly be seen in the first cycle of the voltammogram, which is related to the oxidation of EDOT/NHP and the nucleation of the polymer film.[34,45] The intensities of the redox peaks of the film increased with increasing number of scan cycles due to the regular growth of the PEDOT/NHP film on the surface of the electrode, which implied the formation of the electroactive polymer film on the Pt electrode surface. Further, the continual growth of the PEDOT/NHP film led to the nucleation loop diminishing in all sweeps following the first. Figure 1 shows a single anodic peak at 0.53 V and a cathodic peak at −0.38 V, which were due to the doping/dedoping processes of the PEDOT/NHP film that was formed during the electropolymerization.[46]

Figure 2 illustrates the cyclic voltammogram (for the 10th scan) of the electrodeposition of the EDOT/NHP at different scan rates between 10 and 100 mV s^{-1} with the same measurement conditions applied as for the voltammogram curve (Figure 1). Faraday's law was used to calculate the molar coverage of the PEDOT/NHP films depending on the charge for the final deposition scan, as shown in eq 1.[47]

$$\Gamma = \frac{Q}{nFA} \tag{1}$$

where A represents the PEDOT/NHP electrode area (cm^2), Γ represents the molar coverage (mol cm^{-2}), F is the Faraday constant (C mol^{-1}), Q is the reduction charge, and n is the number of electrons involved.[48] Herein, n is set to be 2.3 and

https://doi.org/10.1021/acsomega.2c02682
ACS Omega 2022, 7, 20405−20419

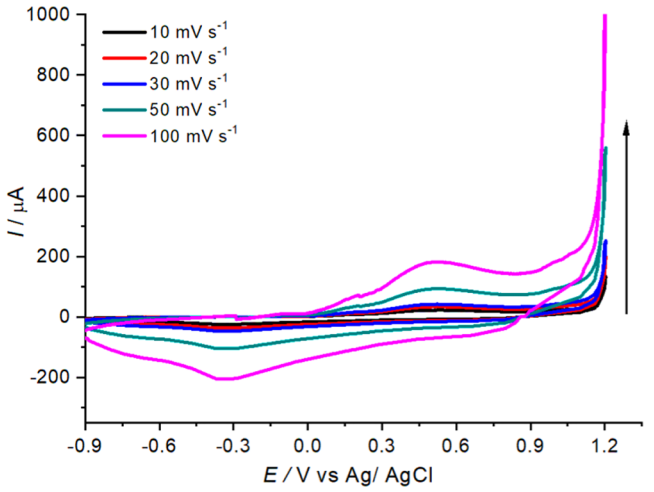

Figure 2. Cyclic voltammogram (for the 10th scan) of the electrodeposition of 10 mM monomer (EDOT/NHP) with 0.1 M TBAP in CH_2Cl_2 solution at different scan rates, ν, 10−100 mV s^{-1}.

the surface area of the PEDOT/NHP-modified electrode is taken to be 0.00785 cm^2. The relative standard deviation of n (RSD%) from three consecutive experiments was estimated, as indicated in Table 1.

Table 1. Charge of Cathodic Peak of PEDOT/NHP at Various Scan Rates (10−100 mV s^{-1})

modified polymer films	scan rate (mV s^{-1})	charge of cathodic peak Q (C)	RSD %, n = 3	coverage area Γ (mol cm^{-2})
poly(EDOT/NHP)	10	1.62×10^{-3}	2.23	9.30×10^{-7}
	20	1.08×10^{-3}	1.56	6.20×10^{-7}
	30	8.92×10^{-4}	2.03	5.11×10^{-7}
	50	7.65×10^{-4}	1.21	4.40×10^{-7}
	100	6.58×10^{-4}	1.65	3.77×10^{-7}

3.2. Electrochemical Characterization of Polymer Films in Monomer-Free Solution. The analysis of the electrochemical properties of the modified films prepared in the previous step using a scan rate of 10 mV s^{-1} (Figure 1) provides information about the electrochemical stability of the polymer-modified electrode. The electrochemical examination was carried out via cyclic voltammetry in an aqueous solution (monomer-free) of TBAP (0.1 M) for PEDT/NHP, as represented in Figure 3. Voltammetric examination revealed one broad redox peak that was possibly due to the diffusion of counterions between the polymer chains. The voltammogram of PEDOT/NHP electrodes shows a broad anodic peak at 0.58 V and a cathodic peak at −0.23 V in a TBAP solution.[49]

Furthermore, the electrochemical features of the polymer film at various scan rates were investigated in an aqueous background electrolyte containing TBAP (0.1 M), as depicted in Figure 3B. From this voltammogram, it can be seen that the current peaks were proportional to the associated scan rates,[37] which supports the supposition that the film has acceptable activity and stability.[38] In addition, there was a linear relationship between oxidation and reduction peak intensities with scan rate, which is referred to as control of surface confinement, as shown in Figure 4.[50]

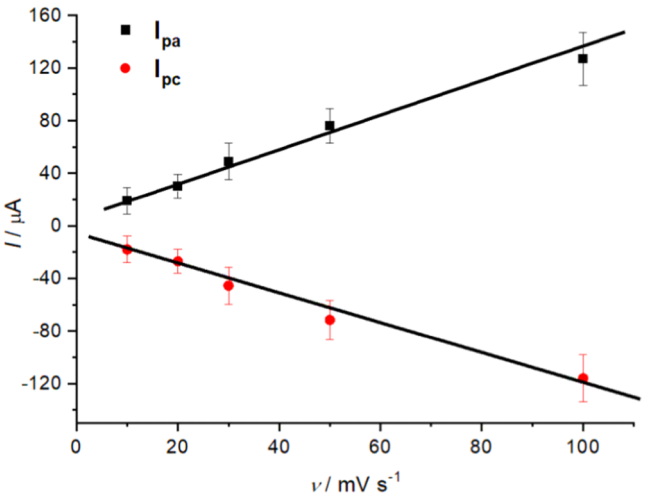

Figure 4. Illustration of the magnitudes of the redox peaks from Figure 3B with various scan rates of 10−100 mV s^{-1}.

The long period electrostability of the PEDOT/NHP-modified electrode prepared at 10 mV s^{-1} was examined via cyclic voltammetry at −0.6 to 0.9 V in the monomer-free

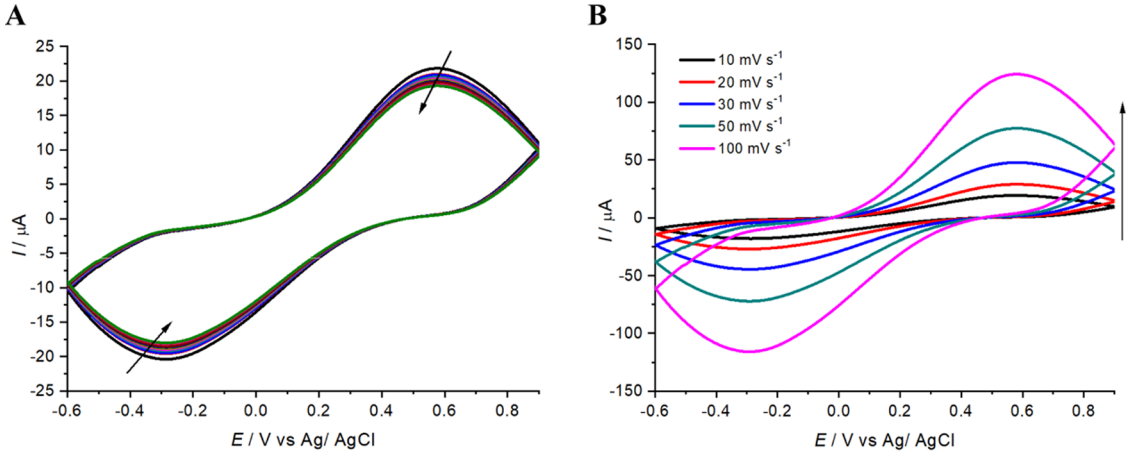

Figure 3. (A) Cyclic voltammograms of poly(EDOT/NHP) electrodes prepared at 10 mV s^{-1} (Figure 1) and acquired in 0.1 M TBAP in the aqueous background electrolyte at −0.6 to 0.9 V. (B) Electrochemical responses of the same poly(EDOT/NHP) film at several scan rates ranging over 10−100 mV s^{-1} in aqueous electrolyte.

https://doi.org/10.1021/acsomega.2c02682
ACS Omega 2022, 7, 20405−20419

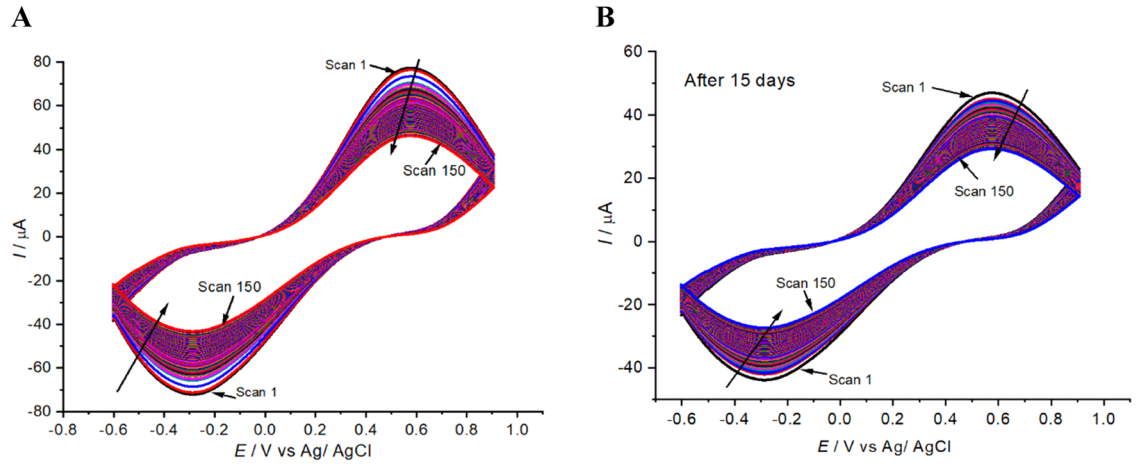

Figure 5. Illustration of the voltammetric response of PEDOT/NHP films prepared at 10 mV s^{-1} for 150 scans and obtained in monomer-free solution at −0.6 to 0.9 V. (A) Immediately after preparation and (B) 15 days after preparation.

aqueous electrolyte. The polymer electrode was studied immediately after preparation, as shown in Figure 5A, and the electrochemical stability of a similarly deposited polymer film was investigated 15 days after deposition, as shown in Figure 5B. The findings support the hypothesis of good electroactivity and stability of the polymer electrode film. The results show that increasing the number of scans during the redox processes for PEDOT/NHP growth exposed to monomer-free electrolyte results in a dwindling in the charge (i.e., from comparing the 1st and 150th cycles).

3.3. FTIR Characterization of EDOT/NHP and PEDOT/NTA Structure and Hydrolysis Study. The chemical compositions of EDOT/NHP and PEDOT/NTA were examined using FTIR spectroscopy (Figure 6). To examine

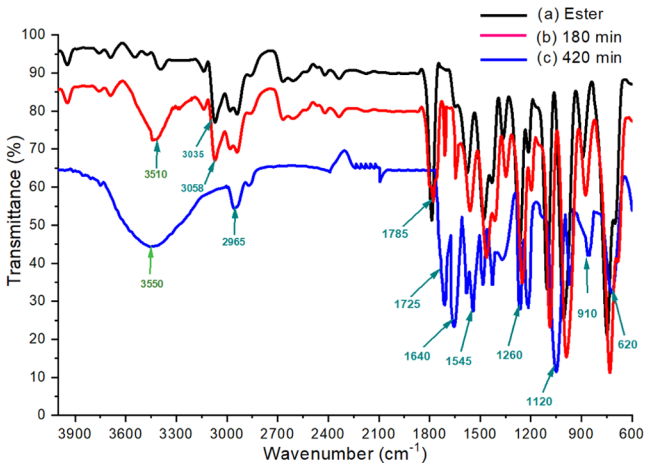

Figure 6. FTIR spectra showing amidation reactions of (a) PEDOT/NHP (black line), (b) film after 180 min (red line), and (c) film after 420 min reaction time (blue line) of PEDOT/NTA.

the hydrolysis of poly(EDOT/NHP) films in N_{α},N_{α}-bis-(carboxymethyl)-L-lysine hydrate (NTA lysine) solution, the experiment compared different reaction times to follow the ratio of the conversion from the ester to the amide form. To perform the hydrolysis procedure, the films were immersed in NTA solution for different lengths of time with simultaneous examination of the reaction using FTIR spectroscopy until the substitution reaction had gone to completion, as shown in Figure 6. FTIR spectroscopy was used to confirm the absence of the C═O group attributed to NHP ester bonds signifying the end of reaction, i.e., confirming that the ester groups had been successfully substituted for amides. FTIR spectroscopy was used to monitor the reaction over time to confirm amide bond formation throughout the polymer surface.[51,52] The poly(EDOT/NHP) film (ester form) showed distinctive sharp bands in the FTIR spectrum at 1790 cm^{-1} that were attributed to the ν(C═O) stretch, as shown in Figure 6. After soaking the NHP ester film in the NTA solution, the C═O stretch was found to shift from 1790 to 1640 cm^{-1}, which was attributed to amide bond formation in the polymer film. Accompanying this conversion in the ester film was the appearance of a broad band at 3550 cm^{-1} due to the ν(O−H) stretch and at 1725 cm^{-1} due to the carbonyl stretch of the COOH groups in the NTA ligand.[53] The FTIR spectrum of PEDOT/NHP shows peaks at 3550 and 2965 cm^{-1} that were assigned to the OH stretch of a carboxylate group and C−H aliphatic stretch, respectively.[54] Further, the bands at 1120, 910, and 620 cm^{-1} were associated with vibrations of the C−S and COC ether groups in 3,4-ethylenedioxythiophene, while the bands at 1640, 1545, and 1260 cm^{-1} were due to the C═C double bound and C−C stretches in the thiophene cyclic group.[55]

3.4. Morphological Characterization of PEDOT/NHP and PEDOT/NTA. The morphologies of the PEDOT-NHP and PEDOT-NTA films were studied via scanning electron microscopy, as shown in Figure 7. The scanning electron microscope images of the PEDOT/NHP film indicated a porous and rough structure. The efficacy and stability of the electropolymer films are strongly related to the morphology of the associated electrode surface. The film was electrodeposited using a voltage range of 0.9−1.3 V vs Ag/AgCl with a scan rate between 10 and 100 mV s^{-1} for 10 scans. Examination of the surface of the polymer shows the growth processes on the electrode surface due to the presence of rough and clustered structures that are joined together like chains.[56] Normally, the electrode surface morphology is strongly influenced by empirical parameters such as temperature, pH, scan rate, solvent, and ions present. SEM images of the PEDOT/NHP electrodes prepared at 10 and 100 mV s^{-1} are illustrated in Figure 7A.

This showed that the use of diverse scan rates led to a change in the size of particles and appearance. The polymer electrode prepared at 100 mV s^{-1} (Figure 7A, right) had a

https://doi.org/10.1021/acsomega.2c02682
ACS Omega 2022, 7, 20405−20419

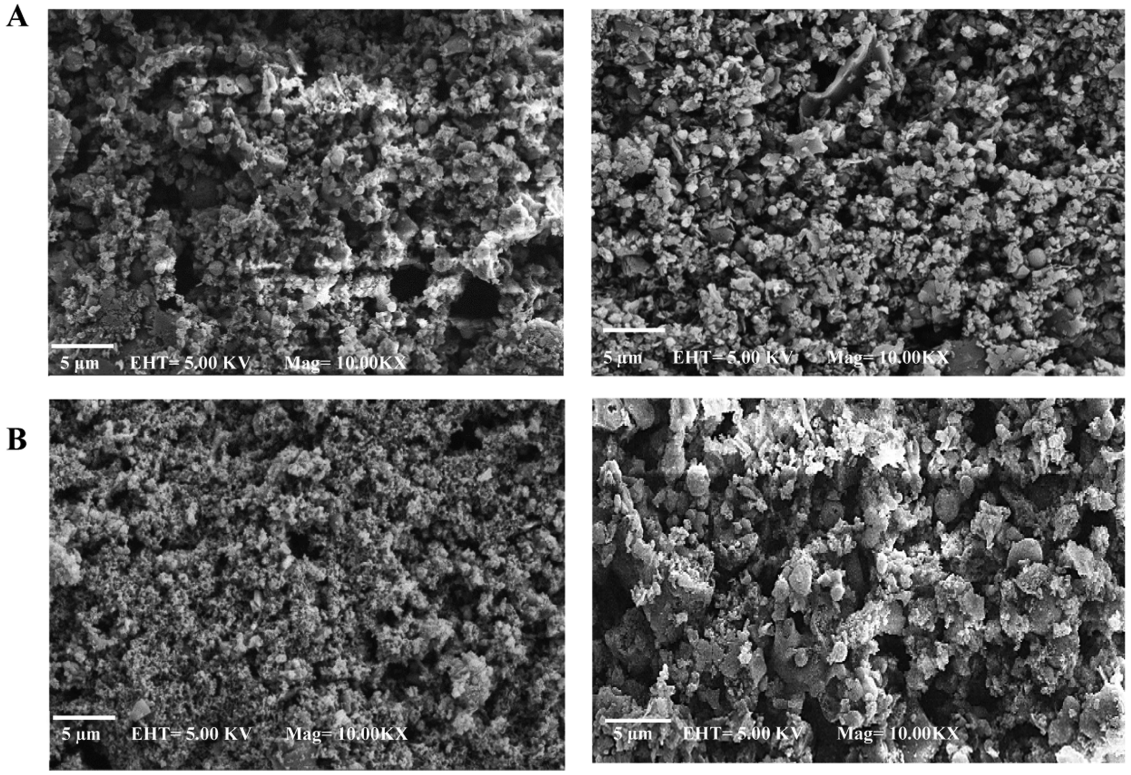

Figure 7. SEM images of polymer surfaces formed using electropolymerization (A) for PEDOT-NHP 10 (left) and 100 (right) mV s^{-1} before hydrolysis and (B) for PEDOT-NTA after hydrolysis for the same films, respectively.

smoother and more uniform appearance with linked particles compared to the film deposited at 10 mV s^{-1}, where the latter had a much rougher morphology with larger-sized particles (Figure 7A, left). The differences in morphology of the surfaces of the polymers were probably due to the rate of nucleation processes and growth of the associated PEDOT films, which are influenced by scan rate. At low scan rates, the rate of the nucleation process for the polymer is slow, and therefore progressive nucleation will be predominant and result in a more uniform, homogeneous crystal surface, while higher scan rates (instantaneous nucleation state) will lead to the formation of larger-sized particles and a coarser morphology. However, the polymer surface of the PEDOT/NTA after hydrolysis in basic media showed a rougher structure as a result of the hydrolysis process and amidation substitution reactions, as shown in Figure 7B.

3.5. Influence of pH. Logically, the oxidation current is influenced by changes in the pH of the electrolyte solution.[57] The electrode response with respect to variation in pH of the medium was investigated, with the objective of achieving the maximum peak current during practical experiments. Three separate solutions containing 100 μg L^{-1} Hg^{2+}, Pb^{2+}, and Zn^{2+} ions in solution at various pHs were utilized for the electrochemical study. The square wave voltammograms showed evident current peak responses for ions in electrolytes with different pHs.[58] Figure 8 illustrates the influence of the pH of the electrolyte on the response of the PEDOT/NTA, and this shows that the peak current increases with pH in the range of 2.0−4.5, at which the peak reaches a maximum, and then declines from pH 5.5 to 9. Therefore, pH 4.5 was selected as the optimum pH for the medium for subsequent experimentation.

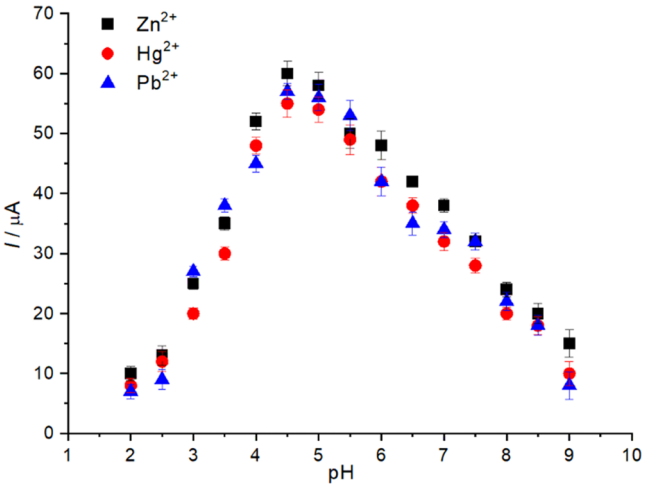

Figure 8. Illustration of peak currents of SWV for Hg^{2+}, Pb^{2+}, and Zn^{2+} ions at various pHs as acquired from PEDOT/NTA-modified electrodes.

3.6. Measurement of Hg, Pb, and Zn Using SWV. The electroanalytical detection of Hg^{2+}-, Pb^{2+}-, and Zn^{2+}-ion concentrations in aqueous solution was achieved using voltammetric measurements. Prior to measurement, the electrode was conditioned using a two-step process. In the first step, the modified polymer PEDOT/NTA electrode was immersed in separate solutions of analytes (Hg^{2+}, Pb^{2+}, and Zn^{2+}) of known concentrations (5−100 μg L^{-1}) at the selected pH of 4.5, where it was envisaged that chemical binding would occur between ions and chelating groups at the polymer electrode surface. In the second step, the PEDOT/NTA electrodes were removed from the analyte media and then

https://doi.org/10.1021/acsomega.2c02682
ACS Omega 2022, 7, 20405−20419

rinsed with pure water before being moved to an electrochemical cell that contains only an acetate solution (buffer). The square wave experiments were accomplished using various Hg^{2+}, Pb^{2+}, and Zn^{2+} concentrations. Figure 9 elucidates the suggested interaction between the PEDOT/NTA ligand groups and the metal ions.

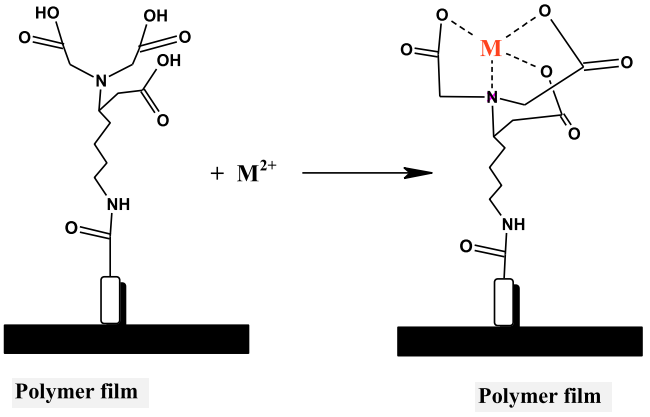

Figure 9. Illustration of the suggested interaction between ligand groups in polymer and Hg^{2+}, Pb^{2+}, and Zn^{2+} ions.

3.7. Determination of Hg, Pb, and Zn Ions. Typical experiment conditions for the detection of Hg^{2+}, Pb^{2+}, and Zn^{2+} ions using the PEDOT/NTA electrode via SWV were investigated individually for each polymer electrode. First, the electroanalytical behavior of the electrode in a blank solution (metal-ion-free) was assessed to ensure that the blank medium did not show any current peak responses in the potential range of −1.3 to 0.7 V, as depicted in Figure 10 (black line). Then, the electroanalytical response of the PEDOT/NTA electrode was determined in buffer solutions (pH 4.5) containing variable concentrations of Hg^{2+}, Pb^{2+}, and Zn^{2+} ions to examine the current responses. In this step, the PEDOT/NTA electrode was washed in ultrapure water and then placed in the buffer electrolyte in the electrochemical cell. The SWV response was recorded for each metal ion. Figure 10 exhibits the current peak for the PEDOT/NTA electrodes placed in 5 $\mu g\ L^{-1}$ solutions of Hg^{2+}, Pb^{2+}, and Zn^{2+} ions. The voltammetric detection of these ion concentrations was evaluated between −1.3 and 0.7 V (vs Ag/AgCl). The interaction between the Hg^{2+}, Pb^{2+}, and Zn^{2+} ions and the polymer electrode surface resulted in a change in the voltammetric responses of the electrode, as shown in Figure 10. The intensity of the oxidation peak increased because of the presence of metal ions in the studied solutions, which likely formed complexes on the modified polymer electrode surface (Figure 10). However, no peak current was registered with the metal-ion-free solution when using the same electrodes (Figure 10A−C).

The correlation coefficients (R^2) and calibration equations were determined for Hg^{2+}, Pb^{2+}, and Zn^{2+} ions as $y = 2.741 + 0.528x$ (x: $\mu g\ L^{-1}$, y: μA), $R^2 = 0.9966$ for Hg^{2+}, $y = 2.857 +$

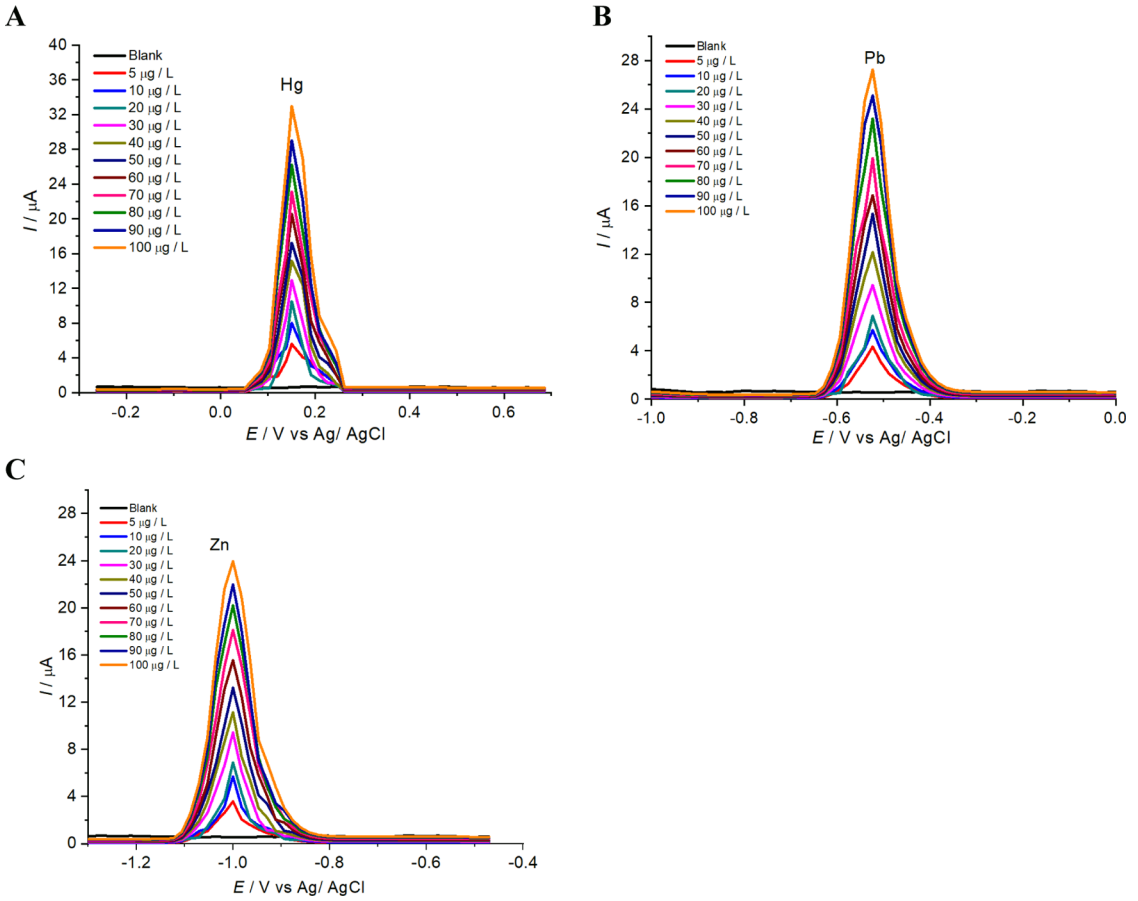

Figure 10. Illustration of curves for SWV for various concentrations (5−100 $\mu g\ L^{-1}$) for (A) Hg^{2+}, (B) Pb^{2+}, and (C) Zn^{2+} ions utilizing PEDOT/NTA-modified electrodes.

https://doi.org/10.1021/acsomega.2c02682
ACS Omega 2022, 7, 20405−20419

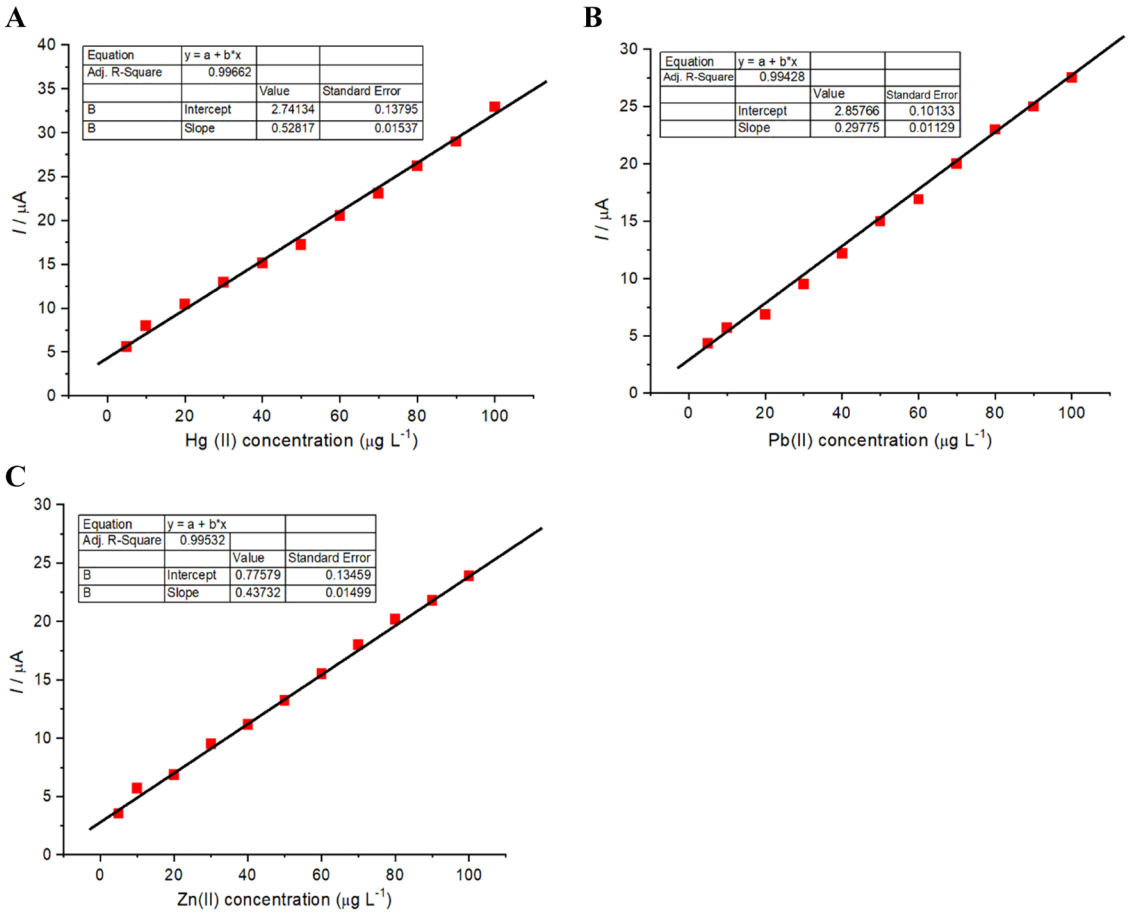

Figure 11. Calibration curves for the measurement of (A) Hg^{2+}, (B) Pb^{2+}, and (C) Zn^{2+} ions for different concentrations (5−100 μg L^{-1}) (obtained from Figure 10) using a PEDOT/NTA electrode.

0.297x (where x: μg L^{-1}, y: μA), R^2 = 0.9942 for Pb^{2+}, and y = 0.775 + 0.437x, R^2 = 0.9953 for Zn^{2+}, respectively, as shown in Figure 11. The limits of detection (LODs) were calculated as 1.73, 2.33, and 1.99 μg L^{-1} for the Hg^{2+}, Pb^{2+}, and Zn^{2+} ions, respectively. This gives a clear indication of the high sensitivity of the novel PEDOT/NTA electrode with regard to the detection of Hg^{2+}, Pb^{2+}, and Zn^{2+} ions. Spatial differences in current peak locations for metal ions provide a precise strategy to detect metal ions, minimizing interfering influences from other metal ions.[59]

Calibrations were determined for the detection of Hg^{2+}, Pb^{2+}, and Zn^{2+} ions in buffer solution at pH 4.5. Square wave voltammograms were recorded using sequential additions of metal ions using a range of concentrations (5−100 μg L^{-1}) at the PEDOT/NTA electrode, as shown in Figure 11. Peak currents emerged at 0.15, −0.52, and −1.0 V for different concentrations of Hg^{2+}, Pb^{2+}, and Zn^{2+} ions, respectively, as illustrated in Figure 10. The findings show that there is an evident linear relationship between the concentration of metal ions and the intensities of the associated current peaks.

3.8. Regeneration of Modified Electrode Using EDTA.

Multiple uses of the PEDOT/NTA electrode to detect Hg^{2+}, Pb^{2+}, and Zn^{2+} ions require that the polymer electrode be repeatedly revived. Reactivation of the PEDOT/NTA electrode was performed by soaking the modified electrode in 0.1 M EDTA solution for 20 min and subsequent washing in deionized water. Figure 12 shows that the findings of the voltammetric study of the PEDOT/NTA electrode after

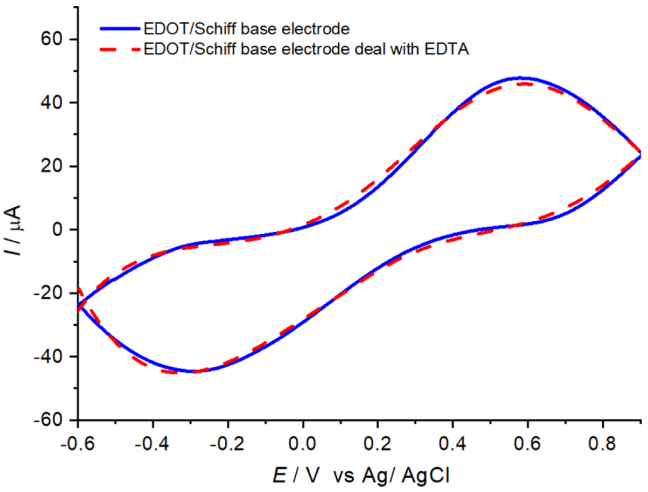

Figure 12. Cyclic voltammetric curve of the PEDOT/NTA-modified electrode (blue curve) and Bu_4NPF_6 electrolyte (red curve) after treatment with 0.1 M EDTA.

reactivation were very closely congruent with the voltammograms of the modified electrode when interacting with the metal ions in solution. Furthermore, the SWV experiment was performed using the reactivated electrode in metal-ion-free solution. This showed that the electrode produced no current peak responses in the applied voltage range, which indicates that the attached ions had completely egressed from the

https://doi.org/10.1021/acsomega.2c02682
ACS Omega 2022, 7, 20405−20419

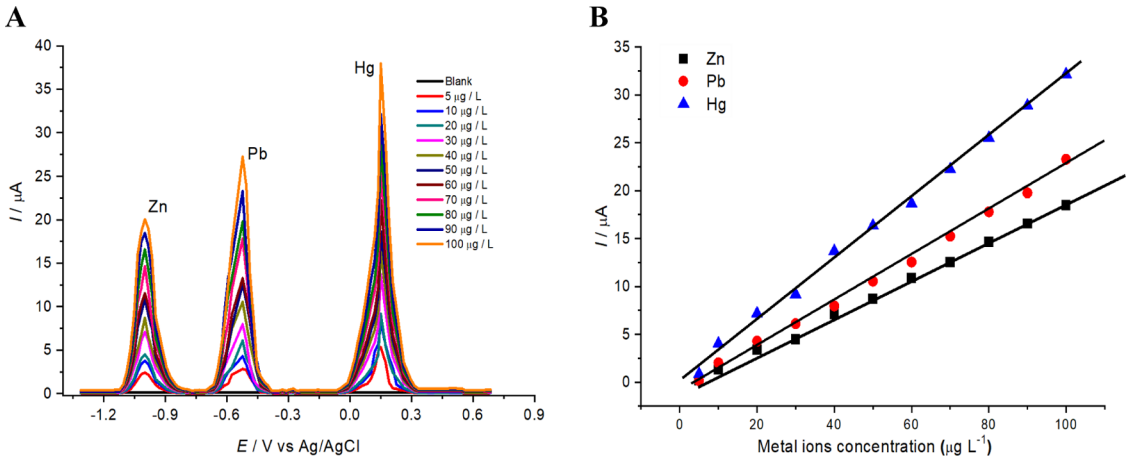

Figure 13. (A) SWV curve responses of the PEDOT/NTA-modified electrode for the simultaneous analysis of Hg^{2+}, Pb^{2+}, and Zn^{2+} ions. (B) Calibration curves in simultaneous detection.

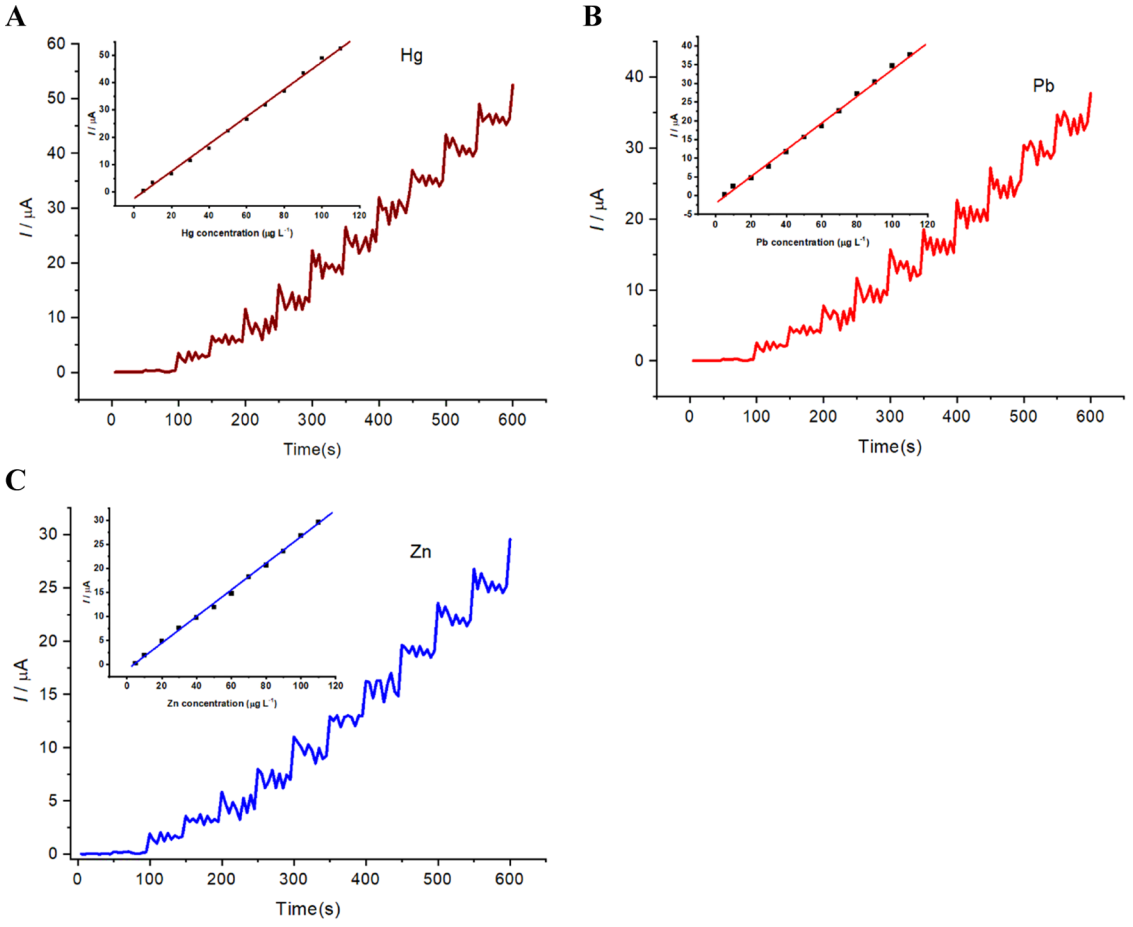

Figure 14. Amperometric $i-t$ curve for the detection of target metal ions at the PEDOT/NTA electrode with graduated addition of ions by 10 μg L^{-1} at regular intervals of 50 s. (A) $i-t$ Curve for Hg^{2+} ions at 0.15 V, (B) $i-t$ curve for Pb^{2+} ions at −0.52 V, (C) $i-t$ curve for Zn^{2+} ions at −1.0 V. The inset plots show the concentration of metal ions vs current.

surface of PEDOT/NTA electrode. As a consequence, a regenerated PEDOT/NTA electrode can be reused for the determination of metal ions without any perceivable effect on the electrode electroactivity.[26]

3.9. Simultaneous Electrochemical Determination of Hg, Pb, and Zn in a Trinary Mixture. The PEDOT-modified film measurements (Figure 13) indicate that the PEDOT/NTA film displays good sensitivity and synchronous responses to Hg^{2+}, Pb^{2+}, and Zn^{2+} ions, with a notable separation of current peaks compared with the blank electrolyte responses, which did not show any responses in the applied potential range of −1.3 to 0.6 V (see Figure 13, black line). The current signals for Hg^{2+}, Pb^{2+}, and Zn^{2+} ions indicated that these ions were efficiently adsorbed onto the polymer surface film (PEDOT/NTA) during the experiment. These findings suggest that the carboxylic groups on the

https://doi.org/10.1021/acsomega.2c02682
ACS Omega 2022, 7, 20405−20419

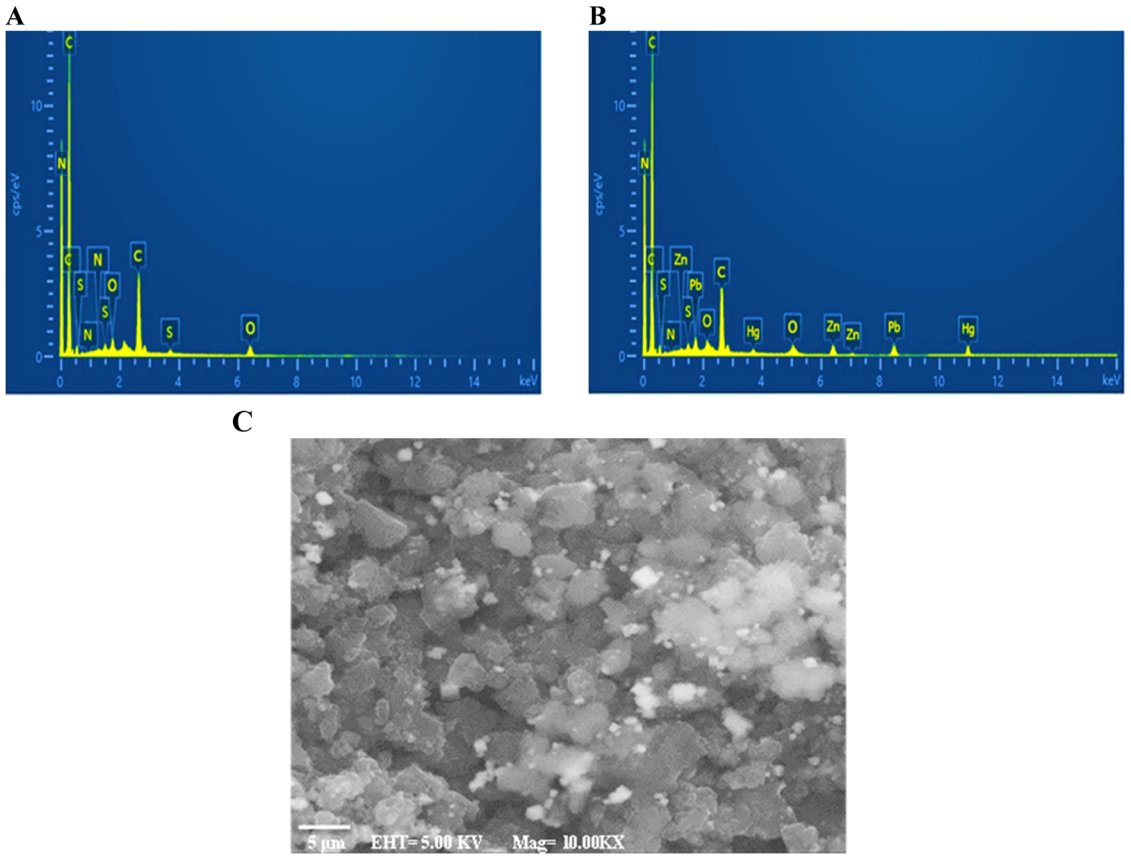

Figure 15. EDX analysis of PEDTA/NTA film (A) before and (B) after adsorption of ions. (C) SEM image of poly(EDTA/NTA) film after adsorption of metal ions.

polymer surface could effectively pick up heavy-metal ions from solution. Detection of metal-ion concentrations was studied in a voltage range between −1.3 and 0.6 V at various concentrations ranging from 5 to 100 μg L^{-1} for Hg^{2+}, Pb^{2+}, and Zn^{2+} ions. Figure 13B depicts square wave voltammograms recorded using a PEDOT/NTA electrode at a scan rate of 5 mV s^{-1}. This finding indicates that current responses increased linearly with increasing concentrations in ternary solutions. These results are in good agreement with the individual species' responses, as can be seen in Figure 10. Therefore, PEDOT-modified electrodes functionalized with the NTA ligand provide sensitivity, selectivity, and simultaneous detection for these three metal ions.[60,61]

3.10. Amperometric Determination of Individual Metal Ions. The amperometric technique was applied to assess the detection of the metal ions (Hg^{2+}, Pb^{2+}, and Zn^{2}) individually, using the modified electrode surface (PEDOT/NTA). Figure 14A displays the amperometric *i*−*t* curve for the PEDOT/NTA electrode acetate solution (buffer) (pH 4.5) to detect Hg ions using a constant voltage of 0.15 V. The polymer electrode shows a current response for each increase of 10 μg L^{-1} mercury. The current signal increase was attained within 5 s for additional increases of 10 Hg^{2+} μg L^{-1} ion in each step with a sample interval of 50 s. The response current was linear from 10 to 100 μg L^{-1} at the modified electrode (PEDOT/NTA) with a correlation coefficient of 0.9971 (inset of Figure 14A). Furthermore, the same conditions for the buffer solution (pH 4.5), sample interval (50 s), and successive additions (10 μg L^{-1}) were applied to assess lead and zinc ions. Figure 14B illustrates a typical *i*−*t* plot for the successive addition of lead ion at −0.52 V. It may be noted that the signal current increased with increasing concentration of Pb^{2+} ions with a correlation coefficient of 0.9975, as shown in the inset of Figure 14B. Finally, the electroanalytical performance of the PEDOT/NTA electrode toward Zn^{2+} detection was measured. Here, the *i*−*t* curve for the Zn^{2+} detection was monitored at a fixed potential of −1.0 V (Figure 14C). The progressive increase in Zn^{2+}-ion concentration shows a proportional current increase with a correlation coefficient of 0.9968, as illustrated in the inset of Figure 14C. The limits of detection (LODs) for the determination of Hg^{2+}, Pb^{2+}, and Zn^{2+} ions were 2.53, 3.24, and 2.89 μg L^{-1}, respectively.

3.11. EDX and SEM Analysis after Adsorption. To allow for the qualitative detection of modified polymer films after metal-ion adsorption and demonstrate the presence of metal in the polymer chains, EDX measurements were performed. The analysis of the polymer films after the adsorption of ions was achieved using EDX measurements. Figure 15A,B depicts EDX spectra of PEDTA/NTA before and after adsorption of ions (Hg^{2+}, Pb^{2+}, and Zn^{2+}), respectively, indicating the presence of these elements within the polymer film as a result of the bonding between the metal ions and carboxylic ligand groups on the surface of the electrode. The analysis indicates the presence of carbon, nitrogen, oxygen, sulfur, mercury, lead, and responses, which shows that the film had bonded with Hg^{2+}, Pb^{2+}, and Zn^{2+} ions in solution. Moreover, the SEM micrograph of poly(EDTA/NTA) after adsorption of metal ions (Hg^{2+}, Pb^{2+}, and Zn^{2+} ions) was measured. Figure 15C depicts the surfaces of the polymer after the adsorption of the ions, from which it may obviously be

https://doi.org/10.1021/acsomega.2c02682
ACS Omega 2022, 7, 20405−20419

noted that the pores and surface of the polymer were covered with metal ions.

3.12. Interference Study. The metal-ion determination employing the PEDOT/NTA electrode can potentially be affected by interfering ions, which could form complexes with the NTA ligands on the modified polymer surface. Therefore, a range of ions (K^+, Na^+, Mg^{2+}, Ca^{2+}, Ba^{2+}, Co^{2+}, Cu^{2+}, Al^{3+}, Fe^{3+}, Ni^{2+}, Cl^-, Ca^{2+}, and NO^{3-}) were added to a mixture containing 25 $\mu g\ L^{-1}$ Pb^{2+}, Zn^{2+}, and Hg^{2+} ions to assess their impact on the current responses of interest. The addition of interfering ions had no tangible effects on the current peaks responses, and the results indicated that the voltammetric responses for Pb^{2+}, Zn^{2+}, and Hg^{2+} were unaffected by most of the interfering species, even when the latter's concentrations exceeded those of the species of interest in the electrolyte, at 25 $\mu g\ L^{-1}$ Hg^{2+}, Pb^{2+}, and Zn^{2+} ions, by 50-fold. However, a minor exception was found in the case of 45-fold concentrations of Co^{2+}, Ni^{2+}, and Cu^{2+}, which were noted to have trivial effects on the detection of Hg^{2+}, Pb^{2+}, and Zn^{2+} ions. This small variation was probably because of competition between ions (Co^{2+}, Ni^{2+}, and Cu^{2+}) and the target ions for receptors/active sites on the electrode surface. Table 2 shows the findings of the interference study using several metal ions on the voltammetric responses of Hg^{2+}, Pb^{2+}, and Zn^{2+}.

Table 2. Interference Analyses for Metal Ions on the Current Peak Responses of Hg^{2+}, Pb^{2+}, and Zn^{2+}

	relative current change (%)		
interfering metal ion	**Hg** $^{2+}$, $\mu g\ L^{-1}$	**Pb**$^{2+}$, $\mu g\ L^{-1}$	**Zn**$^{2+}$, $\mu g\ L^{-1}$
Na	0.22	0.15	0.23
Cu	5.34	4.92	5.02
Ni	−3.93	−4.62	−4.95
Co	4.32	3.56	4.89
Al	−0.46	−0.44	−0.45
Fe	1.21	2.12	2.54
K	0.26	0.32	0.35
Ca	−0.72	−0.65	−0.52
Mg	1.10	1.19	0.98
Ba	1.57	1.05	1.09
NO_3	0.37	0.95	1.02
Cl	0.82	0.13	0.98
Ca	−4.23	−3.86	−4.08

3.13. Repeatability/Reproducibility Tests. The repeatability of polymer electrode behavior was examined under optimized conditions using 30 $\mu g\ L^{-1}$ Hg^{2+}, Pb^{2+}, and Zn^{2+}. Five successive experiments were carried out using the same PEDOT/NTA electrode; the calculated relative standard deviations (RSD) were 3.8, 3.1, and 2.7% for Hg^{2+}, Pb^{2+}, and Zn^{2+}, respectively. Furthermore, the reproducibility study of the PEDOT/NTA film involved the synthesis of five PEDOT/NTA electrodes, which were then applied to the detection of 30 $\mu g\ L^{-1}$ Hg^{2+}, Pb^{2+}, and Zn^{2+}. The RSDs of the PEDOT/NTA films were 2.9, 3.02, and 2.8% for Hg^{2+}, Pb^{2+}, and Zn^{2+}, respectively. This result indicated that the prepared PEDOT/NTA-modified electrodes showed good repeatability and reproducibility.

3.14. Comparison with Previous Studies. The results of the examination emphasized that the PEDOT/NTA-modified electrode exhibits suitable reliability and eligibility to be used for the determination of Hg^{2+}-, Pb^{2+}-, and Zn^{2+}-ion concentrations. The electroanalytical responses of the PEDOT/NTA electrodes employed in this study were compared with the prior literature on the determination of Hg^{2+}, Pb^{2+}, and Zn^{2+}, as shown in Table 3.

3.15. Determination of Hg, Pb, and Zn Ions in Real-World Samples. Real-world samples were used to evaluate the ability of our sensor to detect target metal ions in tap water. To assess the practicality of the modified electrode sensor, it was assessed for the detection of Hg^{2+}, Pb^{2+}, and Zn^{2+} ions in a tap water sample spiked with 50 $\mu g\ L^{-1}$ of the aforementioned metals. Prior to spiking, Hg^{2+}, Pb^{2+}, and Zn^{2+} concentrations were below detection in this water sample. The experimental findings are presented in Table 4, indicating good agreement between "added" and "measured" concentration, suggesting that the PEDOT/NTA-modified electrode sensor is applicable for "real-world" practical applications.

Table 4. Determination of Hg^{2+}, Pb^{2+}, and Zn^{2+} in Natural Water Samples

natural water sample	**Hg** $^{2+}$, $\mu g\ L^{-1}$	**Pb**$^{2+}$, $\mu g\ L^{-1}$	**Zn**$^{2+}$, $\mu g\ L^{-1}$
added	50	50	50
found	45.9	48.2	47.8

Table 3. Comparison of the Electroanalytical Responses of the Polymer Electrode with Previous Studies

polymer electrodes	methods	analytes	detection limit	references
phthalocyanine film	DPV	Hg	4×10^{-9} M	62
poly(3,4-thylenedioxythiophene)/black TiO_2 composites	SWASV	Pb, Cd	0.15 $\mu g\ L^{-1}$	63
poly(1,5-diaminonaphthalene)	SWASV	Pb	0.3 $\mu g\ L^{-1}$	64
(EDTA-CPME)	SWV	Pb, Cu and Hg	6.0×10^{-10}, 2.0×10^{-10}, and 5.0×10^{-10} M	65
Langmuir−Blodgett films	SWASV	Hg	0.1 ppm	66
EDTA bonded 30,40-diamino-2,20;50,200-terthiophene on GCE	SWASV	Hg, Pb and Cu	6.0×10^{-10}, 2.0×10^{-10}, 5.0×10^{-10} M	67
CNSs/PPy/SPE	SWASV	Hg and Pb	0.0128 and 0.0014 nM	68
L-cysteine-doped PPy		Hg	2042.7 mg g^{-1}	69
GCE/(PEDOT)	LSASV	Pb and Cd	1.47 and 1.15 $\mu g\ mL^{-1}$	16
EDTA_PANI/SWCNTs	DPV	Cu, Pb and Hg	0.08 mM, 1.65 and 0.68 mM	49
poly(1,8-diaminonaphthalene)	ASV	Cd, Pb and Cu	19, 30 and 6 ng L^{-1}	60
PEDOT:PSS/GC	chronoamperometry	Pb	0.19 nmol L^{-1}	70
phthalocyanine electrode	voltammetry and amperometry	Pb	37 nmol L^{-1}	71

https://doi.org/10.1021/acsomega.2c02682
ACS Omega 2022, 7, 20405−20419

4. CONCLUSIONS

This project focuses on the fabrication of functionalized films for use as electrochemical sensors for metal ions in aqueous solution. A novel electrochemical sensor for metal ions, using the modified polymer, was successfully fabricated using electrochemical techniques. PEDOT functionalized with the NHP group was electrodeposited onto a platinum surface electrode via cyclic voltammetry, followed by a hydrolysis step to remove NHP groups and insert the NTA groups within the polymer matrix. The subsequent PEDOT/NTA was characterized via cyclic voltammetry (CV), Fourier transform infrared (FTIR) spectroscopy, scanning electron microscopy (SEM), and energy-dispersive X-ray (EDX) spectroscopy. The effects of scan rate on the electrochemical properties of the polymer electrode were also investigated. The novel PEDOT/NTA film was assessed for the detection of Hg^{2+}, Pb^{2+}, and Zn^{2+} ions in aqueous solution. Hg^{2+}, Pb^{2+}, and Zn^{2+} ions were determined individually and simultaneously via the SWV technique using the new modified polymer (PEDOT/NTA) moieties. The PEDOT/NTA film displayed good sensitivity during detection experiments for trace amounts of Hg^{2+}, Pb^{2+}, and Zn^{2+}, showing very low limits of detection of 1.73 $\mu g\ L^{-1}$ for Hg^{2+}, 2.33 $\mu g\ L^{-1}$ for Pb^{2+}, and 1.99 $\mu g\ L^{-1}$ for Zn^{2+}.

AUTHOR INFORMATION

Corresponding Authors

Mohammed Q. Mohammed − *Department of Chemistry, College of Education for Pure Sciences, University of Basrah, Basrah 61001, Iraq*; Email: mahammed.qasim@uobasrah.edu.iq

Hasan F. Alesary − *Department of Chemistry, College of Science, University of Kerbala, Karbala 56001, Iraq*; orcid.org/0000-0002-3116-5145; Email: hasan.f@uokerbala.edu.iq

Authors

Jasim M. S. Alshawi − *Department of Chemistry, College of Education for Pure Sciences, University of Basrah, Basrah 61001, Iraq*

Hani K. Ismail − *Department of Chemistry, Faculty of Science and Health, Koya University, Koya KOY45 Kurdistan Region − F.R., Iraq*; orcid.org/0000-0001-5407-1806

Stephen Barton − *School of Life Sciences, Pharmacy and Chemistry, Kingston University London, Kingston-Upon-Thames KT1 1LQ Surrey, U.K.*; orcid.org/0000-0002-9661-8416

Complete contact information is available at: https://pubs.acs.org/10.1021/acsomega.2c02682

Notes

The authors declare no competing financial interest.

ACKNOWLEDGMENTS

The authors thank the Universities of Basrah, Koya, and Kerbala for providing the required materials and instruments for this work. The authors acknowledge Dr. Mark Watkins (University of Leicester) for helping with and proofreading the manuscript.

REFERENCES

(1) Ding, S.; Ali, A.; Jamal, R.; Xiang, L.; Zhong, Z.; Abdiryim, T. An Electrochemical Sensor of Poly (EDOT-Pyridine-EDOT)/Graphitic Carbon Nitride Composite for Simultaneous Detection of Cd^{2+} and Pb^{2+}. *Materials* **2018**, *11*, 702.

(2) Mohammed, M. Q.; Ismail, H. K.; Alesary, H. F.; Barton, S. Use of a Schiff base-modified conducting polymer electrode for electrochemical assay of Cd (II) and Pb (II) ions by square wave voltammetry. *Chem. Pap.* **2022**, *76*, 715−729.

(3) Ariño, C.; Núria, S.; Díaz-Cruz, J. M.; Miquel, E. Voltammetric determination of metal ions beyond mercury electrodes. A review. *Anal. Chim. Acta* **2017**, *990*, 11−53.

(4) Mahesar, S. A.; Sherazi, S. T. H.; Niaz, A.; Bhanger, M. I.; Uddin, S.; Rauf, A. Simultaneous Assessment of Zinc, Cadmium, Lead and Copper in Poultry Feeds by Differential Pulse Anodic Stripping Voltammetry. *Food Chem. Toxicol.* **2010**, *48*, 2357−2360.

(5) Koelmel, J.; Amarasiriwardena, D. Imaging of Metal Bioaccumulation in Hay-Scented Fern (Dennstaedtia Punctilobula) Rhizomes Growing on Contaminated Soils by Laser Ablation ICP-MS. *Environ. Pollut.* **2012**, *168*, 62−70.

(6) Massadeh, A. M.; Alomary, A. A.; Mir, S.; Momani, F. A.; Haddad, H. I.; Hadad, Y. A. Analysis of Zn, Cd, As, Cu, Pb, and Fe in Snails as Bioindicators and Soil Samples near Traffic Road by ICP-OES. *Environ. Sci. Pollut. Res.* **2016**, *23*, 13424−13431.

(7) Palacios, M. A.; Zhuo, W.; Victor, A.; Grigory, V.; Pavel, A. Rational Design of a Minimal Size Sensor Array for metal ion detection. *J. Am. Chem. Soc.* **2008**, *130*, 10307−10314.

(8) Siraj, K.; Kitte, S. A. Analysis of Copper, Zinc and Lead Using Atomic Absorption Spectrophotometer in Ground Water of Jimma Town of Southwestern Ethiopia. *Int. J. Chem. Anal. Sci.* **2013**, *4*, 201−204.

(9) Ding, Q.; Li, C.; Wang, H.; Xu, C.; Kuang, H. Electrochemical Detection of Heavy Metal Ions in Water. *Chem. Commun.* **2021**, *57*, 7215.

(10) Numan, A.; Gill, A. A. S.; Rafique, S.; Guduri, M.; Zhan, Y.; Maddiboyina, B.; Li, L.; Singh, S.; Dang, N. N. Rationally Engineered Nanosensors: A Novel Strategy for the Detection of Heavy Metal Ions in the Environment. *J. Hazard. Mater.* **2021**, *409*, No. 124493.

(11) Liang, Y.; Mingsheng, M.; Faqiang, Z.; Feng, L.; Tan, L.; Zhifu, L.; Yongxiang, L. Wireless Microfluidic Sensor for Metal Ion Detection in Water. *ACS Omega* **2021**, *6*, 9302−9309.

(12) Bansod, B.; Kumar, T.; Thakur, R.; Rana, S.; Singh, I. A Review on Various Electrochemical Techniques for Heavy Metal Ions Detection with Different Sensing Platforms. *Biosens. Bioelectron.* **2017**, *94*, 443−455.

(13) Power, A. C.; Gorey, B.; Chandra, S.; Chapman, J. Carbon Nanomaterials and Their Application to Electrochemical Sensors: A Review. *Nanotechnol. Rev* **2018**, *7*, 19−41.

(14) Naveen, M. H.; Gurudatt, N. G.; Shim, Y.-B. Applications of Conducting Polymer Composites to Electrochemical Sensors: A Review. *Appl. Mater. Today* **2017**, *9*, 419−433.

(15) Park, M.-O.; Noh, H.; Park, D.; Yoon, J.; Shim, Y. Long-life Heavy Metal Ions Sensor Based on Graphene Oxide-anchored Conducting Polymer. *Electroanalysis* **2017**, *29*, 514−520.

(16) Anandhakumar, S.; Mathiyarasu, J.; Phani, K. L. N.; Yegnaraman, V. Simultaneous Determination of Cadmium and Lead Using PEDOT/PSS Modified Glassy Carbon Electrode. *Am. J. Anal. Chem.* **2011**, *02*, 470.

(17) Gumpu, M. B.; Sethuraman, S.; Krishnan, U. M.; Rayappan, J. B. B. A Review on Detection of Heavy Metal Ions in Water−an Electrochemical Approach. *Sens. Actuators, B* **2015**, *213*, 515−533.

(18) Shen, L.-L.; Zhang, G.-R.; Li, W.; Biesalski, M.; Etzold, B. J. M. Modifier-Free Microfluidic Electrochemical Sensor for Heavy-Metal Detection. *ACS Omega* **2017**, *2*, 4593−4603.

(19) Günay, K. A.; Schüwer, N.; Klok, H.-A. Synthesis and Post-Polymerization Modification of Poly (Pentafluorophenyl Methacrylate) Brushes. *Polym. Chem.* **2012**, *3*, 2186−2192.

(20) Jurjevec, S.; Antoine, D.; Ema, Ž.; Sebastijan, K. An environmentally benign post-polymerization functionalization strategy towards unprecedented poly(vinylamine) polyHIPEs. *Polym. Chem.* **2021**, *12*, 1155.

https://doi.org/10.1021/acsomega.2c02682
ACS Omega 2022, 7, 20405−20419

(21) Koberstein, J. T. Molecular Design of Functional Polymer Surfaces. *J. Polym. Sci., Part B: Polym. Phys.* **2004**, *42*, 2942−2956.
(22) Anantha-Iyengar, G.; Shanmugasundaram, K.; Nallal, M.; Lee, K.-P.; Whitcombe, M. J.; Lakshmi, D.; Sai-Anand, G. Functionalized Conjugated Polymers for Sensing and Molecular Imprinting Applications. *Prog. Polym. Sci.* **2019**, *88*, 1−129.
(23) Kumar, P.; Joseph, A.; Ramamurthy, P. C.; Subramanian, S. Lead Ion Sensor with Electrodes Modified by Imidazole-Functionalized Polyaniline. *Microchim. Acta* **2012**, *177*, 317−323.
(24) Manisankar, P.; Vedhi, C.; Selvanathan, G.; Arumugam, P. Differential Pulse Stripping Voltammetric Determination of Heavy Metals Simultaneously Using New Polymer Modified Glassy Carbon Electrodes. *Microchim. Acta* **2008**, *163*, 289−295.
(25) Fang, Y.; Bo, C.; Jianzhi, H.; Lishi, W. Ultrasensitive electrochemical sensor for simultaneous determination of cadmium and lead ions based on one-step co-electropolymerization strategy. *Sens. Actuators, B* **2019**, *284*, 414−420.
(26) Mohammed, M. Q. Patterned Functionalisation of Conducting Polymer Films, Thesis; University of Leicester, 2018.
(27) AL-Refai, H. H.; Ganash, A. A.; Hussein, M. A. Polythiophene and Its Derivatives−Based Nanocomposites in Electrochemical Sensing: A Mini Review. *Mater. Today Commun.* **2020**, No. 101935.
(28) Song, Y.; Bian, C.; Hu, J.; Li, Y.; Tong, J.; Sun, J.; Gao, G.; Xia, S. Porous Polypyrrole/Graphene Oxide Functionalized with Carboxyl Composite for Electrochemical Sensor of Trace Cadmium (II). *J. Electrochem. Soc.* **2019**, *166*, B95.
(29) Hui, Y.; Bian, C.; Xia, S.; Tong, J.; Wang, J. Synthesis and Electrochemical Sensing Application of Poly (3, 4-Ethylenedioxythiophene)-Based Materials: A Review. *Anal. Chim. Acta* **2018**, *1022*, 1−19.
(30) Ismail, H. K.; Alesary, H. F.; Mohammed, M. Q. Synthesis and Characterisation of Polyaniline and/or MoO_2/Graphite Composites from Deep Eutectic Solvents via Chemical Polymerisation. *J. Polym. Res.* **2019**, *26*, 65.
(31) Alesary, H. F.; Ismail, H. K.; Khudhair, A. F.; Mohammed, M. Q. Effects of Dopant Ions on the Properties of Polyaniline Conducting Polymer. *Oriental J. Chem.* **2018**, *34*, 2525−2533.
(32) Chakraborty, C.; Singh, P.; Maji, S. K.; Malik, S. Conjugated Polyfluorene-Based Reversible Fluorescent Sensor for Cu (II) and Cyanide Ions in Aqueous Medium. *Chem. Lett.* **2013**, *42*, 1355.
(33) Alesary, H. F.; Ismail, H. K.; Mohammed, M. Q.; Mohammed, H. N.; Abbas, Z. K.; Barton, S. A comparative study of the effect of organic dopant ions on the electrochemical and chemical synthesis of the conducting polymers polyaniline, poly (o-toluidine) and poly (o-methoxyaniline). *Chem. Pap.* **2021**, *75*, 5087−5101.
(34) Hillman, A. R.; Ryder, K. S.; Ismail, H. K.; Unal, A.; Voorhaar, A. Fundamental Aspects of Electrochemically Controlled Wetting of Nanoscale Composite Materials. *Faraday Discuss.* **2017**, *199*, 75−99.
(35) Yasri, N. G.; Sundramoorthy, A. K.; Chang, W.-J.; Gunasekaran, S. Highly Selective Mercury Detection at Partially Oxidized Graphene/Poly (3, 4-Ethylenedioxythiophene): Poly (Styrenesulfonate) Nanocomposite Film-Modified Electrode. *Front. Mater.* **2014**, *1*, 33.
(36) Fathi, A. M.; Mandour, H. S. Electrosynthesized Conducting Poly (1, 5-Diaminonaphthalene) as a Corrosion Inhibitor for Copper. *Polym. Bull.* **2020**, *77*, 3305−3324.
(37) Zhang, W.; Chen, X.; Zhang, G.; Wang, S.; Zhu, S.; Wu, X.; Wang, Y.; Wang, Q.; Hu, C. Conducting Polymer/Silver Nanowires Stacking Composite Films for High-Performance Electrochromic Devices. *Sol. Energy Mater. Sol. Cells* **2019**, *200*, No. 109919.
(38) Han, Y.; Dai, L. Conducting Polymers for Flexible Supercapacitors. *Macromol. Chem. Phys.* **2019**, *220*, No. 1800355.
(39) Ibanez, J. G.; Rincón, M. E.; Gutierrez-Granados, S.; Chahma, M.; Jaramillo-Quintero, O. A.; Frontana-Uribe, B. A. Conducting Polymers in the Fields of Energy, Environmental Remediation, and Chemical−Chiral Sensors. *Chem. Rev.* **2018**, *118*, 4731−4816.
(40) Pascual, V. H.; Otero, T. F.; Schumacher, J. Biomimetic Reactions in Conducting Polymers for Artificial Muscles: Sensing Working Conditions. In *Bioinspiration, Biomimetics, and Bioreplication 2017*, International Society for Optics and Photonics, 2017; Vol. *10162*, p 101620D.
(41) Lange, U.; Roznyatovskaya, N. V.; Mirsky, V. M. Conducting Polymers in Chemical Sensors and Arrays. *Anal. Chim. Acta* **2008**, *614*, 1−26.
(42) Glidle, A.; Hillman, A. R.; Ryder, K. S.; Smith, E. L.; Cooper, J. M.; Dalgliesh, R.; Cubitt, R.; Geue, T. Metal Chelation and Spatial Profiling of Components in Crown Ether Functionalised Conducting Copolymer Films. *Electrochim. Acta* **2009**, *55*, 439−450.
(43) Glidle, A.; Bailey, L.; Hadyoon, C. S.; Hillman, A. R.; Jackson, A.; Ryder, K. S.; Saville, P. M.; Swann, M. J.; Webster, J. R. P.; Wilson, R. W.; Cooper, J. M. Temporal and Spatial Profiling of the Modification of an Electroactive Polymeric Interface Using Neutron Reflectivity. *Anal. Chem.* **2001**, *73*, 5596−5606.
(44) Li, Y.; He, J.; Zhang, K.; Liu, T.; Hu, Y.; Chen, X.; Wang, C.; Huang, X.; Kong, L.; Liu, J. Super Rapid Removal of Copper, Cadmium and Lead Ions from Water by NTA-Silica Gel. *RSC Adv.* **2019**, *9*, 397−407.
(45) Popov, A.; Brasiunas, B.; Mikoliunaite, L.; Bagdziunas, G.; Ramanavicius, A.; Ramanaviciene, A. Comparative Study of Polyaniline (PANI), Poly (3, 4-Ethylenedioxythiophene)(PEDOT) and PANI-PEDOT Films Electrochemically Deposited on Transparent Indium Thin Oxide Based Electrodes. *Polymer* **2019**, *172*, 133−141.
(46) Mohammed, M. Q.; Jassem, A. M.; Al-Shawi, J. M. S.; Alesary, H. F. Comparative Electrochemical Behavior of Poly (3-Aminobenzoic Acid) Films in Conventional and Non-Conventional Solvents. *AIP Conf. Proc.* **2020**, *2290*, No. 030029.
(47) Sapstead, R. M.; Corden, N.; Hillman, A. R. Latent Fingerprint Enhancement via Conducting Electrochromic Copolymer Films of Pyrrole and 3, 4-Ethylenedioxythiophene on Stainless Steel. *Electrochim. Acta* **2015**, *162*, 119−128.
(48) Brown, R. M.; Hillman, A. R. Electrochromic Enhancement of Latent Fingerprints by Poly (3, 4-Ethylenedioxythiophene). *Phys. Chem. Chem. Phys.* **2012**, *14*, 8653−8661.
(49) Deshmukh, M. A.; Celiesiute, R.; Ramanaviciene, A.; Shirsat, M. D.; Ramanavicius, A. EDTA_PANI/SWCNTs Nanocomposite Modified Electrode for Electrochemical Determination of Copper (II), Lead (II) and Mercury (II) Ions. *Electrochim. Acta* **2018**, *259*, 930−938.
(50) Ismail, H. K. Novel Battery Chemistries Using Electrically Conducting Polymers Synthesised from Deep Eutectic Solvents and Aqueous Solutions; Thesis, University of Leicester, 2017.
(51) Xie, Y.; Zhang, S.-H.; Jiang, H.-Y.; Zeng, H.; Wu, R.-M.; Chen, H.; Gao, Y.-F.; Huang, Y.-Y.; Bai, H.-L. Properties of Carbon Black-PEDOT Composite Prepared via in-Situ Chemical Oxidative Polymerization. *e-Polymers* **2019**, *19*, 61−69.
(52) Hong, C. K.; Ko, H. S.; Han, E. M.; Park, K. H. Electrochemical Properties of Electrodeposited PEDOT Counter Electrode for Dye-Sensitized Solar Cells. *Int. J. Electrochem. Sci.* **2015**, *10*, 5521−5529.
(53) Khan, S.; Majid, A.; Raza, R. Synthesis of PEDOT: PPy/AC Composite as an Electrode for Supercapacitor. *J. Mater. Sci.: Mater. Electron.* **2020**, *31*, 13597−13609.
(54) Mantione, D.; Casado, N.; Sanchez-Sanchez, A.; Sardon, H.; Mecerreyes, D. Easy-to-make Carboxylic Acid Dioxythiophene Monomer (ProDOT-COOH) and Functional Conductive Polymers. *J. Polym. Sci., Part A: Polym. Chem.* **2017**, *55*, 2721−2724.
(55) Mantione, D.; Marquez, A. V.; Cruciani, F.; Brochon, C.; Cloutet, E.; Hadziioannou, G. Synthesis of Carboxyl-EDOT as a Versatile Addition and Additive to PEDOT: PSS. *ACS Macro Lett.* **2019**, *8*, 285−288.
(56) Sheng, Y.; Qian, W.; Huang, J.; Wu, B.; Yang, J.; Xue, T.; Ge, Y.; Wen, Y. Electrochemical Detection Combined with Machine Learning for Intelligent Sensing of Maleic Hydrazide by Using Carboxylated PEDOT Modified with Copper Nanoparticles. *Microchim. Acta* **2019**, *186*, 543.
(57) Pandey, S. K.; Sachan, S.; Singh, S. K. Ultra-Trace Sensing of Cadmium and Lead by Square Wave Anodic Stripping Voltammetry Using Ionic Liquid Modified Graphene Oxide. *Mater. Sci. Energy Technol.* **2019**, *2*, 667−675.

https://doi.org/10.1021/acsomega.2c02682
ACS Omega 2022, 7, 20405−20419

(58) Korolkov, I. V.; Zhumanazar, N.; Gorin, Y. G.; Yeszhanov, A. B.; Zdorovets, M. V. Enhancement of Electrochemical Detection of Pb2+ by Sensor Based on Track-Etched Membranes Modified with Interpolyelectrolyte Complexes. *J. Mater. Sci.: Mater. Electron.* **2020**, *31*, 20368−20377.
(59) Dang, V. H.; Yen, P. T. H.; Giao, N. Q.; Phong, P. H.; Ha, V. T. T.; Duy, P. K.; Hoeil, C. A Versatile Carbon Fiber Cloth-supported Au Nanodendrite Sensor for Simultaneous Determination of Cu (II), Pb (II) and Hg (II). *Electroanalysis* **2018**, *30*, 2222−2227.
(60) Hassan, K. M.; Elhaddad, G. M.; AbdelAzzem, M. Voltammetric Determination of Cadmium (II), Lead (II) and Copper (II) with a Glassy Carbon Electrode Modified with Silver Nanoparticles Deposited on Poly (1, 8-Diaminonaphthalene). *Microchim. Acta* **2019**, *186*, 440.
(61) Sengupta, P.; Pramanik, K.; Sarkar, P. Simultaneous Detection of Trace Pb (II), Cd (II) and Hg (II) by Anodic Stripping Analyses with Glassy Carbon Electrode Modified by Solid Phase Synthesized Iron-Aluminate Nano Particles. *Sens. Actuators, B* **2021**, *329*, No. 129052.
(62) Manjunatha, P.; Shambhulinga, A.; CP, K.; Prabhu, V.; ASajjan, M.; Lokesh, K. S. Nanomolar detection of mercury(II) using electropolymerized phthalocyanine film. *Electrochim. Acta* **2021**, *367*, No. 137519.
(63) Yu, Z.; Jamal, R.; Zhang, R.; Zhang, W.; Yan, Y.; Liu, Y.; Ge, Y.; Abdiryim, T. PEDOT-Type Conducting Polymers/Black TiO2 Composites for Electrochemical Determination of Cd^{2+} and Pb^{2+}. *J. Electrochem. Soc.* **2020**, *167*, No. 067514.
(64) Nguyen, M. T. T.; Nguyen, H. L.; Nguyen, D. T. Poly(1,5-Diaminonaphthalene)-Modified Screen-Printed Device for Electrochemical Lead Ion Sensing. *Adv. Polym. Technol.* **2021**, *2021*, No. 6637316.
(65) Rahman, M. A.; Won, M.-S.; Shim, Y.-B. Characterization of an EDTA Bonded Conducting Polymer Modified Electrode: Its Application for the Simultaneous Determination of Heavy Metal Ions. *Anal. Chem.* **2003**, *75*, 1123−1129.
(66) Ng, S. C.; Zhou, X. C.; Chen, Z. K.; Miao, P.; Chan, H. S. O.; Li, S. F. Y.; Fu, P. Quartz Crystal Microbalance Sensor Deposited with Langmuir− Blodgett Films of Functionalized Polythiophenes and Application to Heavy Metal Ions Analysis. *Langmuir* **1998**, *14*, 1748−1752.
(67) Rahman, M. D.; Kumar, P.; Park, D.-S.; Shim, Y.-B. Electrochemical Sensors Based on Organic Conjugated Polymers. *Sensors* **2008**, *8*, 118−141.
(68) Lo, M.; Diaw, A. K. D.; Gningue-Sall, D.; Aaron, J.-J.; Oturan, M. A.; Chehimi, M. M. Tracking Metal Ions with Polypyrrole Thin Films Adhesively Bonded to Diazonium-Modified Flexible ITO Electrodes. *Environ. Sci. Pollut. Res.* **2018**, *25*, 20012−20022.
(69) Ballav, N.; Das, R.; Giri, S.; Muliwa, A. M.; Pillay, K.; Maity, A. L-Cysteine Doped Polypyrrole (PPy@L-Cyst): A Super Adsorbent for the Rapid Removal of Hg^{+2} and Efficient Catalytic Activity of the Spent Adsorbent for Reuse. *Chem. Eng. J.* **2018**, *345*, 621−630.
(70) Yasri, N. G.; Halabi, A. J.; Istamboulie, G.; Noguer, T. Chronoamperometric Determination of Lead Ions Using PEDOT: PSS Modified Carbon Electrodes. *Talanta* **2011**, *85*, 2528−2533.
(71) Veeresh, A. S.; Shambhulinga, A. M.; Nemakal, M. P.; Keshavananda, P. L.; Koodlur, S. Nanomolar detection of lead using electrochemical methods based on a novel phthalocyanine. *Inorg. Chim. Acta* **2020**, *506*, No. 119564.

https://doi.org/10.1021/acsomega.2c02682
ACS Omega 2022, 7, 20405−20419